

A STEREO PCM TAPE DECK EMPLOYING STATIONARY HEAD

By

Kunimaro Tanaka and Katsuhito Uetake
Mitsubishi Electric Corporation
Hyogo, Japan

presented at the
57th Convention
May 10 - 13, 1977
Los Angeles

AES

AN AUDIO ENGINEERING SOCIETY PREPRINT

This preprint has been reproduced from the author's advance manuscript, without editing, corrections or consideration by the Review Board. For this reason there may be changes should this paper be published in the Audio Engineering Society Journal. Additional preprints may be obtained by sending request and remittance to the Audio Engineering Society, Room 449, 60 East 42nd Street, New York, N.Y. 10017.

©Copyright 1977 by the Audio Engineering Society. All rights reserved. Reproduction of this preprint, or any portion thereof, is not permitted without direct permission from the publication office of the Society.



A STEREO PCM TAPE DECK EMPLOYING STATIONARY HEAD

Kunimaro Tanaka
Katsuhito Uetake

Products Development Lab.
Mitsubishi Electric Corp.

Abstract

Quality sound reproduction is a human desire, and yet the problem has been in the limitations of conventional tape recorders. PCM can exclude all their drawbacks. However, its frequency range broadens about 100 times. Our OPEN REEL 9 TRACK DECK (6.3mm tape, 38 cm/sec) can cover this employing high density recording technique. This paper mainly describes its magnetic recording and error control.

1. Introduction

There have been remarkable developments in recent audio equipment in response to the requirements of high fidelity sound reproduction. Of the whole range of this equipment, from the microphone input to the eventual speaker output, only the tape recorder, despite the fact that it is indispensable, still presents serious problems with respect to high fidelity reproduction. Major problems include narrow dynamic range, tape hiss, print through, harmonic distortion and multi-copy degradation, arising from the properties of the magnetic tape.

It is, however, well known that these problems can be solved by digital techniques such as PCM recording, and these have recently been introduced to audio systems^{1,2,3}. PCM recording offers two significant advantages: one is the independence of the PCM signal of noise and non-linearity in the recording medium made possible by correct decoding when the '0' and '1' pulse states are correctly identified; the other is that time-base errors (wow and flutter, etc.) can be readily eliminated by an electronic compensator.

Despite its obvious advantages, PCM recording requires a frequency range many times wider than that of the base band. It is also inherently subject to serious degradation of sound quality in the face of drop-outs. These disadvantages caused the PCM recorders developed by several manufacturers to be both complex and bulky. This is the reason for PCM recorders failure to secure widespread use, despite their excellent points.

In the authors' conception, PCM recorders should be as convenient to operate as conventional tape recorders. Accordingly a major effort has been directed at the realization of such a simple PCM tape recorder, employing the stationary head and conventional tape deck mechanism (6.3mm tape width, and 38 cm/sec tape speed) of other recorders, and offering the same tape splicing, editing and monitoring functions.

2. Outline of the PCM Tape Recorder

2-1 The tape pattern format

A normal low tape speed magnetic recorder would not normally be expected to be able to record PCM signals because of their expanded frequency range. This problem may be overcome by the introduction of multi-track recording. According to this method, the input audio signal is encoded by PCM and allocated to a number of tracks in parallel.

There are two methods of performing this allocation⁴. One is the bit distribution method, in which each bit of the pulse code signal is allocated to a different track. The other is the frame distribution method, in which a single frame, containing all the bits of the corresponding pulse code signal(s), is allocated to a single track. Our PCM recorder employs the latter method for the following reasons.

- (1) Sample errors caused by drop-outs can be reduced, and
- (2) The number of tracks can be chosen independently of the number of code bits.

A single frame, on our scheme, consists of four samples for the left channel, four for the right, a 15-bit frame synchronizing code and a 16-bit cyclic redundancy check (CRC) as illustrated in Fig. 1. At least nine tracks are required to record a PCM signal at a tape speed of 38 cm/sec with acceptable bit error rate and permissible recording density. The individual frames are therefore allocated over nine tracks as shown in Fig. 2.

2-2 Signal processing

The system specifications of this recorder are given in Table 1, and the block diagram in Fig. 3. The upper part of the block diagram illustrates the recording section and the lower part shows the reproduction section. An audio signal applied to the input terminals passes through a low pass filter (LPF) which serves to reject aliasing noise. The output signal from the

LPF is sampled and encoded using 13-bit PCM. The sampling frequency is set at 48 kHz in order to secure an audio frequency bandwidth of 20 kHz. Quality sound reproduction is said to require a dynamic range of about 80 dB, and this requirement is met by our recorder.

The ratio of signal (S) to quantum noise (N_Q) is given by

$$S/N_Q = 6 \times N + 1.8 \text{ (dB)}$$

where N is the number of coding bits. For an S/N_Q of about 80 dB, N should be chosen as 13.

As mentioned above, one frame of serial high speed PCM signal consists of four left channel and four right channel samples, the synchronizing code and CRC. This leads to a bit rate for the high speed PCM signal which reaches 1.6 Mbits/sec, and inevitably requires multi-track recording at a tape speed of 38 cm/sec.

The frame distributor has a total of nine memories, each of which corresponds to a single recording track. The serial high speed PCM signal is sequentially read in frame by frame. While one memory works on read-in, others serve for the read-out of parallel low speed PCM signals at a rate one-ninth of that of read-in. This reduces the bit rate of the corresponding parallel low speed PCM signal to 180 kbits/sec. The read-out signal is coded by a modified FM (MFM) system and write compensation is applied before it is recorded on the magnetic tape. In the playback mode the reproduced MFM signal is demodulated to the parallel low speed PCM signal and is then fed to a jitter compensator.

The signal reproduced from the tape is subject to dynamic errors caused by irregularities in the transport system, the so-called 'wow and flutter,' and also static errors arising from head misalignment. These two types of error are eliminated by the jitter compensator. The principle of operation is as follows.

The jitter compensator has two memories for each track. While the low speed PCM signal is clocked into the first memory from each track by the reproduced bit synchronizing pulse, the high speed PCM signal is clocked out of the second memory by the crystal oscillator synchronizing pulse, at a speed of some nine times that of the clock-in pulse. The result is to ensure that the jitter compensator output gives exactly the same output as the original serial high speed PCM signal, free from

time base error. The reproduced high speed PCM signal is then checked at the CRC, and any errors detected are corrected by the appropriate interpolation. The resulting PCM signal is then decoded and sent out through the LPF, eliminating spurious components in the audio signal.

2-3 Structure and mechanism

Fig. 4 shows the appearance of the PCM recorder. The PCM recorder splits into three sections for convenient handling. The top unit holds the tape deck, the middle unit holds the circuitry, and the lower unit carries the power supplies.

The tape transport is essentially similar to those of conventional analog tape recorders, using 6.3 mm tape and 38 cm/sec tape speed. Capstan speed is phase-locked so as not to overload the memory of the jitter compensator.

2-4 Performance data

The performance specifications are shown in Table 2, and Fig. 5 illustrates the frequency characteristics and noise level of this PCM recorder and of a conventional tape recorder. The uppermost curve corresponds to the output level for 3% distortion. The flat frequency characteristics and low noise level of the PCM recorder are clearly evident. Fig. 6 indicates that the distortion levels of the PCM recorder are about one tenth those of the analog tape recorder. There is also no amplitude fluctuation in the output signal, as shown in Fig. 7, and as would be expected from the principles of the PCM signal.

3. Characteristics of the Magnetic Recording Channels

3-1 Performance of the recording channel without drop-out

Recording 180 kbits/sec at 38 cm/sec corresponds to a density of 472 bit/mm per track on the magnetic tape. Table 3 shows the specifications of the tape and head used to attain this recording density. Resolution is about 65%. Peak shift is $\pm 25\%$ without write compensation, reducing to $\pm 12.5\%$ with it for a (110) pattern, which is the worst case for recording.

Noise in the reproduced MFM signal cause peak shift-induced bit errors. The peak detection method is employed in this MFM demodulator as shown in Fig. 8. Let V be the reproduced signal peak-to-peak voltage, and V_n be the rms noise voltage, with S the maximum peak shift caused by pulse crowding and

and jitter measured at the input of the zero cross detector. Assuming that the reproduced signal is sinusoidal, the signal voltage V_w at the edge of the window is

$$V_w = V \sin \frac{\pi}{4} (1 - 4S)$$

as illustrated in Fig. 9, because the window is $\pm T/4$. Assuming noise is Gaussian, the bit error rate p caused by noise is

$$p = \text{erfc} \left(\frac{V_w}{2V_n} \right) = \text{erfc} \left[\sin \frac{\pi}{4} (1 - 4S) \times \frac{V}{2V_n} \right]$$

where

$$\text{erfc}(v) = \frac{1}{\sqrt{2\pi}} \int_v^{\infty} \exp(-\frac{1}{2}t^2) dt \approx \frac{1}{(\sqrt{2\pi})v} \exp(-\frac{v^2}{2})$$

$V = 3V_{p-p}$, $V_n = 0.1 V_{rms}$, and $S = 0.125\%$ from our measurements.

Consequently, p becomes about 10^{-8} , very much lower than the bit rate error caused by drop-outs as mentioned below.

3.2 Performance of the recording channel during drop-outs

Drop-outs may be classified into two types: permanent and temporary. Permanent drop-out arises from high edges, wrinkles induced by improper handling, and coating nodules and holes caused by defective manufacturing processes. However, it is possible to eliminate tapes with these causes of permanent drop-outs by inspection. Temporary drop-out, on the other hand, is mainly caused by fragments of magnetic particles and air-borne dust. It can be reduced by tape cleaning, but it cannot be eliminated.

Drop-outs cause the separation of the tape and the tape head, so that contact is lost, and spacing losses increase. The magnitude of the influence of a drop-out, therefore, depends upon the frequency of the recorded signal, as is evident from the equation for spacing loss. The spacing loss, L_s , is⁵

$$L_s \approx 54.6 \frac{d}{\lambda} \text{ (dB)}$$

where d is the distance between the head and the recording medium, and λ is the recorded wavelength. Fig. 10 gives an example of peak shift and resolution during a drop-out. Recorded signal is alternately (1111) 16 bits and (1010) 16 bits. The (1111) signal corresponds to 90 kHz (2F pattern) and (1010) corresponds to 45 kHz (1F pattern) because they are coded by MFM. The horizontal axis of Fig. 10 is time. Fig. 10b shows

the output of the main amplifier, and reveals the change of resolution with time during a drop-out, while Fig. 10d identifies the elements in the photograph 10b. In Fig. 10b, the high amplitude sections correspond to the 1F pattern, and the low amplitude sections correspond to the 2F pattern. The ratio of the amplitude of the 1F pattern to the 2F pattern is the resolution. Fig. 10a illustrates the change of peak shift vs. time during a drop-out caused by pulse crowding and noise. Fig. 10c explains the details of Fig. 10a. The vertical axis of Fig. 10a is the pulse interval, and the upper line corresponds to T (the time for a bit cell) and the lower line corresponds to $2T$. T s and $2T$ s appear alternately and T appears when the 2F pattern is reproduced, and vice versa.

The peak shift increases during the drop-out because of the reduced resolution and increased noise level. When an asymmetrical pattern such as (110) is recorded, the corresponding peak shift will be cumulative to that due to the drop-out, so that the influence of drop-outs differs in accordance with the recorded pattern. In general, even less serious drop-outs will cause bit errors, if the margin of peak shift is less than in this example.

Fig. 11 shows the extent to which the number of drop-outs increases with the reduced level of drop-out. The number of minor drop-outs is much greater than that of major ones, and the number of bit errors will therefore increase if the recording density is high. Measurements of bit error rate run typically at $10^{-6} \sim 10^{-5}$, although they differ not only from tape to tape but also from place to place in the same tape. Minor bit errors tend to occur together in bursts, with the average burst length being about 55 bits.

4. Error Control

4-1 Subjective impairment of error concealment

Error concealment is essential in view of the rather poor 'transmission line characteristics' of the high density digital recording used, and the resultant bit errors in the recorded PCM signal. Various kinds of error concealment have been proposed, but subjective evaluations of error concealment as applied to burst errors were hitherto lacking. We have attempted the necessary subjective evaluations.

Fig. 12 shows the maximum number of frames that can be extrapolated at zero order without being perceived vs. the mean time between error frames when there are burst errors. The level of

subjective impairment depends largely on the kind of source. The silent pauses between words and phrases in an announcer's speech (for example in a weather forecast) are least susceptible to the noise which arises from zero order extrapolation, and such noise is then most imperceptible. Zero order extrapolation of four samples lies at the barely perceptible limit if one frame error occurs in a second.

On the other hand, the longer the CRC code, the greater the possibility of detecting a burst error: since the length of the CRC increases with longer code words when redundancy is held constant, a longer code word is desirable in this respect. However, the longer code word will give rise to more noise when it is extrapolated at zero order. Consideration of the above factors lies behind the choice of four samples, a 16-bit CRC, and error concealment by interpolation, for the frames of this PCM tape recorder.

4-2 Probability of error detection

The CRC is extremely effective in detecting burst errors⁶. When an $(n - r)$ bit data block is coupled with a CRC of r bits, the performance is as follows.

- (1) A burst error with length not greater than r bits can be detected perfectly.
- (2) When a burst has a length of $r + 1$, or more than $r + 1$, the probability of a decoding error will be $2^{-(r-1)}$ and 2^{-r} respectively.
- (3) When a generating polynomial is divisible by $(x + 1)$, odd number bit errors are perfectly detected. Since the generating polynomial used in this recorder is $x^{16} + x^{12} + x^5 + 1$, so that odd number bit errors are detected.

Let P_e be defined as the probability of decoding an error, P_d the probability of detecting an error, and P_c the probability of correct decoding. These terms will, of course, be related by the expression

$$P_c + P_d + P_e = 1 \quad (1)$$

In the following calculation, a random error is assumed for simplicity. Let $P(m, n)$ be defined as the probability of m errors occurring in an n -bit block, and p be a bit error rate.

$$P(m, n) = \binom{n}{m} p^m (1 - p)^{n-m}$$

then

$$P_c = P(0,n) = (1-p)^n \approx 1-np, \text{ where}$$

$p \ll 1$ (which holds true for most cases), then from (1),

$$P_d + P_e = 1 - P_c \approx np$$

Since $P_e \ll P_d$, $P_d \approx np$ (2)

$$P_e = 2^{-(r+1)} [(n-r)p]^2 \quad (\text{Appendix}) \quad (3)$$

P_d and P_e vs. p are illustrated in Fig. 13 for $n = 135$ and $r = 16$.

$N_f \times P_d$ is the number of occasions on which click noise arises due to interpolation, where N_f is the number of frames to be recorded per second, and in this case takes the value 1200. From equation (2), P_d is about $10^{-3} - 10^{-4}$ for $n = 135$ with $p = 10^{-5} - 10^{-6}$, giving interpolation noise between 1.6 and 16 times per second.

However, the above calculation overestimates the incidence of such noise because most errors are burst errors of average length about 50 bits, as mentioned in paragraph 3-2, and of the 50 about half will probably be correct within the burst. This reduces the number of frame errors to one 25th of the above calculation in practice, with a mean time between clicks of approximately 1.6 to 16 sec. These figures are in close agreement with measured values. As will be evident from Fig. 12, interpolation noise is quite imperceptible. Should an error fail to be detected, however, the analog output level of the D/A converter assumes some independent value, and in the worst case will produce a quite unacceptable sound. Since, according to equation (3), P_e is of the order of $10^{-11} - 10^{-13}$, a single decoding error click can be expected in anything from a three-month to a 25-year period if the PCM is played continuously for long periods.

5. The Future

Although the PCM tape recorder employing a stationary head features simple tape transport mechanism and easy operation, the number of MFM circuits, jitter compensators, and frame distributors must equal the number of tracks, so it suffers from the disadvantages of high circuit cost and large size. However, future progress in high density magnetic recording will enable the number of tracks to be reduced, and circuit

costs will be reduced by going to LSIs. We may therefore expect the PCM recorder to replace the analog recorder, which is currently the weak link in the chain of audio reproduction, in the not-too-distant future.

Acknowledgements

Contributions to the achievements described in this paper were made by T. Tsuiki in the area of error control, and by T. Ishibashi and T. Furukawa in the area of magnetic recording. The authors wish to thank Dr. Jingo Hara for permission to publish this paper.

Appendix: The Probability of Not Detecting a Frame Error

Let us assume that the code word and the cyclic redundancy check consist of n and r bits respectively. In order to calculate the probability of failing to detect a frame error, the probability of the occurrence of a burst error with more than $r + 1$ bits in an n -bit code word, P_B , must be calculated. When an i -bit burst error occurs in a code word, at least both the first and last bits of the burst must be in error (although all the bits between them may be correct), and the rest of the bits in the code word must be correct, as shown in Fig. 14. Therefore the probability $P_b(i)$ that an i -bit burst error occurs in an n -bit code word is

$$P_b(i) = (n - i + 1)p^2(1 - p)^{n-i}$$

where p is a bit error rate.

Therefore

$$P_B = \sum_{i=r+1}^n (n - i + 1)p^2(1 - p)^{n-i}$$

Let $k = i - r - 1$

$$P_B = \sum_{k=0}^{n-r-1} (n - r - k)p^2(1 - p)^{n-r-k-1}$$

$$= 1 - (1 - p)^{n-r}[1 + (n - r)p]$$

Let $p \ll 1$ (this holds true in most cases), then

$$P_B \approx 1 - [1 - (n - r)p][1 + (n - r)p] = [(n - r)p]^2$$

$$P_e' \approx 2^{-r}P_B = 2^{-r}[(n - r)p]^2$$

where P_e' is the probability of failing to detect a burst of

more than $(r+1)$ bits.

As mentioned in paragraph 4-2, odd number bit errors are perfectly detected. Therefore P_e , the decoding error, is

$$P_e = 2^{-1}P_e' = 2^{-(r+1)} [(n-r)p]^2$$

References

- (1) Hiroshi Iwamura, Hideki Hayashi, Atsushi Miyashita, and Takeaki Anazawa, Nippon Columbia Company Ltd., Tokyo, Japan. "Pulse-Code-Modulation Recording System" JOURNAL OF THE AUDIO ENGINEERING SOCIETY, September 1973, Volume 21, Number 7
- (2) A.H. Jones, F.A. Bellis, BBC Research Development "Digitas Stereo Sound Recorder" WIRELESS WORLD, September 1972.
- (3) N. Sato, Oki Electric Industry Company Limited, Tokyo, Japan, "PCM Recorder: A New Type of Audio Magnetic Tape Recorder" JOURNAL OF THE AUDIO ENGINEERING SOCIETY, September 1973, Volume 21, Number 7
- (4) Yasunori Kanazawa, Masuo Umemoto, Koichi Tomatsuri, and Hisashi Nakamura, "PCM Sound Recorder Using Fixed Magnetic Heads" THE JOURNAL OF THE ACOUSTICAL SOCIETY OF JAPAN, Oct. 1975 Vol.31, No.10
- (5) C.D. Mee, THE PHYSICS OF MAGNETIC RECORDING, North Holland Publishing Co., 1964.
- (6) R.W. Lucky, J. Saltz and E.J. Weldon, Jr., PRINCIPLES OF DATA COMMUNICATION, McGraw-Hill, Inc., 1968.

Frame synchronizing code

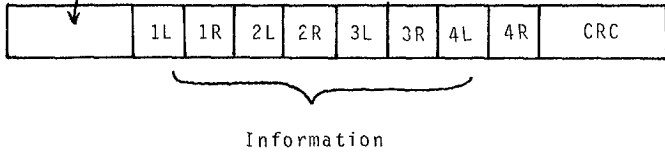


Fig. 1 Frame Construction

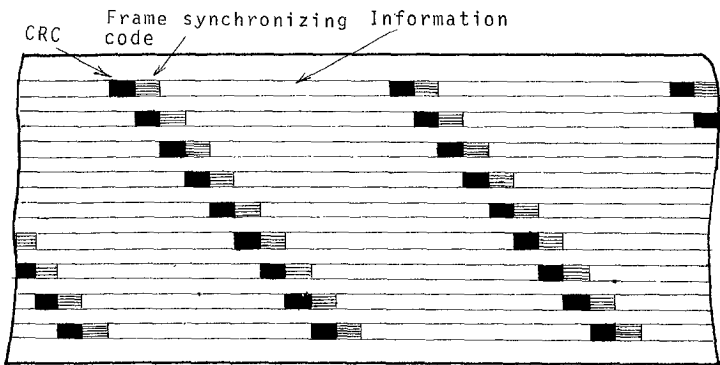


Fig. 2 Distribution of PCM Signal

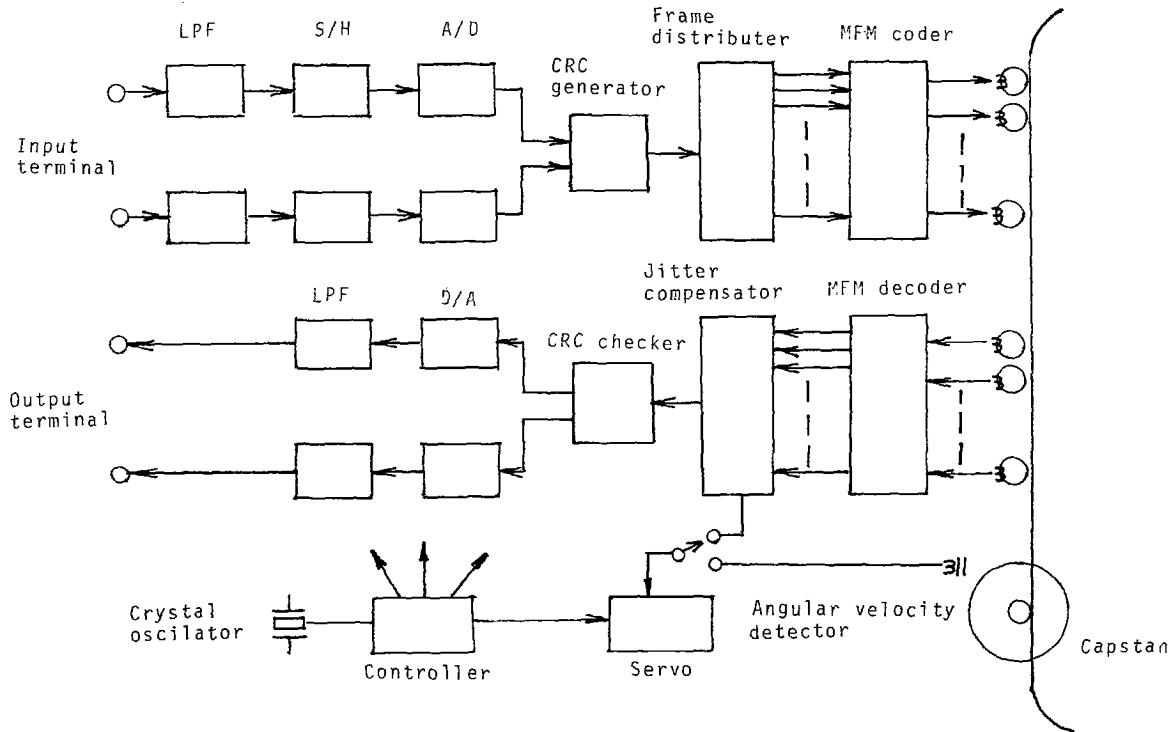


Fig. 3 Block Diagram of the PCM Recorder

Coding	13-bit Natural Binary
Sampling Frequency	48kHz
Tape	6.3mm High Density Tape
Tape Speed	38cm/sec
Number of Tracks	9
Recording Modulation	MFM
Recording Density	472 bit/mm
Error Concealment	Interpolation

Table 1 System Specifications

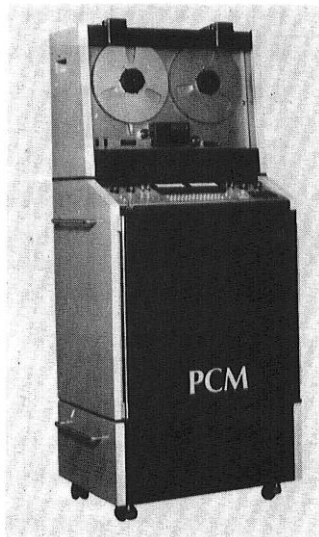
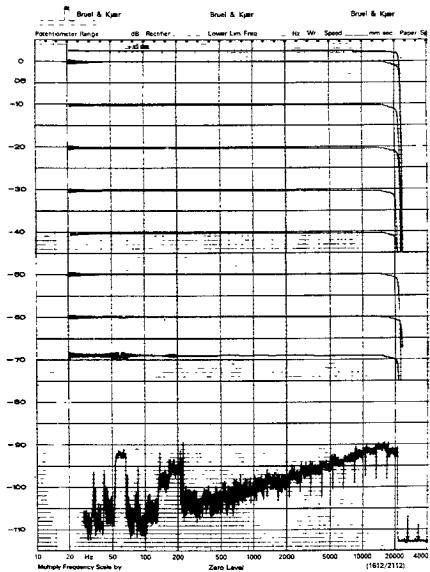


Fig. 4 External Appearance

Audio Channels	2
Bandwidth	DC - 20 KHz (± 0.5 dB)
Dynamic Range	85dB (Weighting Curve A)
Total Distortion	0.01% (Full Scale)
Cross-talk	Less than noise level
Wow and Flutter	Equivalent to Crystal Oscillator Accuracy

Table 2 Performance Specifications

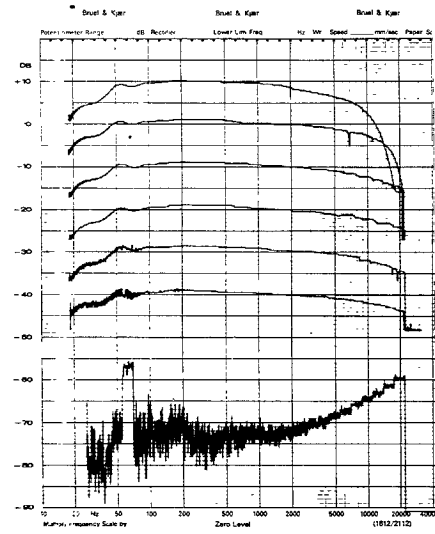
Level



Frequency

PCM Recorder

Level



(Hz)

Frequency

Analog Recorder

Fig. 5 Output and Noise Level vs. Frequency

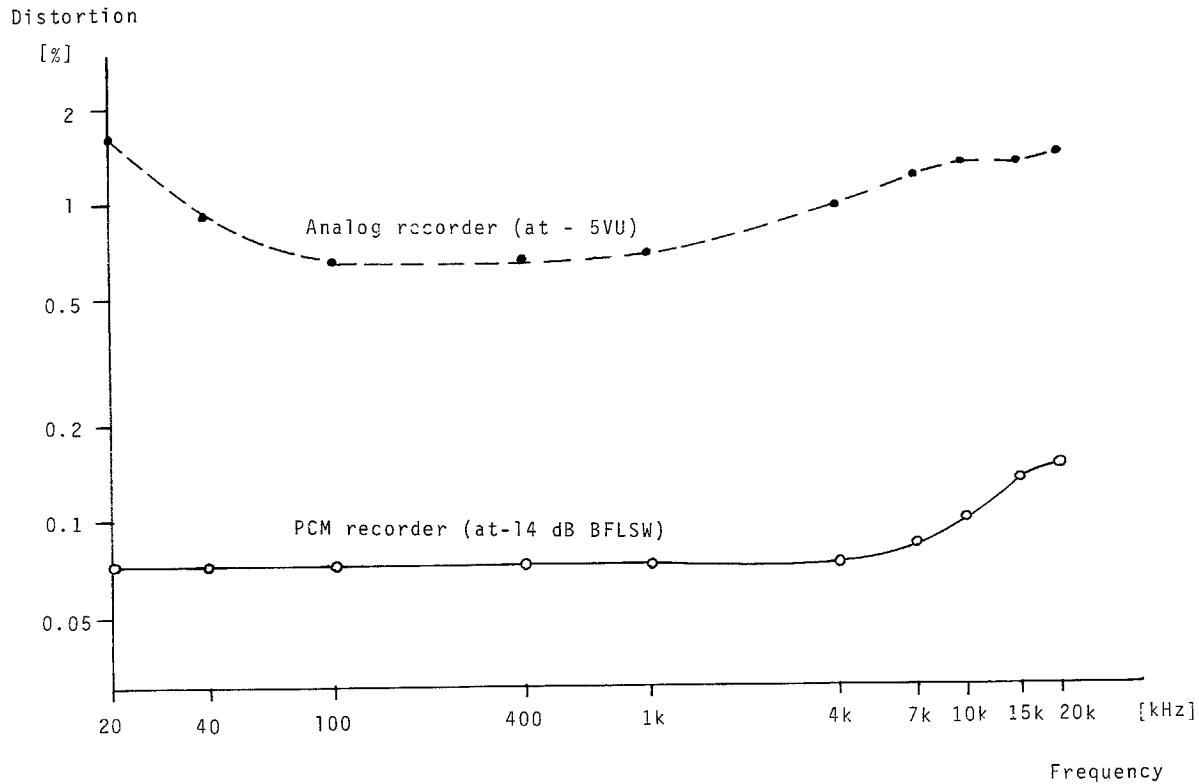
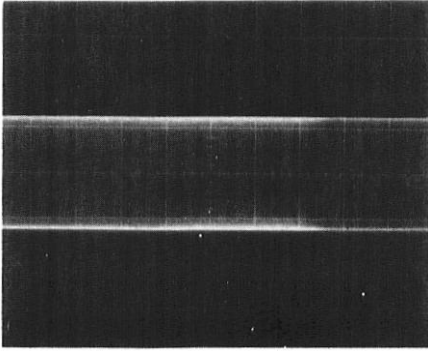
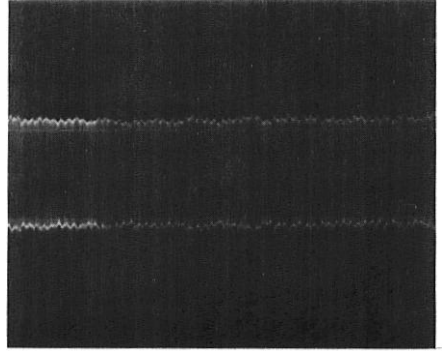


Fig. 6 Distortion vs. Frequency



PCM Recorder



Analog Recorder

Fig 7 Amplitude (recording signal 20kHz)

Tape	Intrinsic Coercivity	680 Oe
	Retentivity	1200 gauss
	Coating Thickness	28 μm
Head	Precision Ferrite Head	

Table 3 Specification of Tape and Head

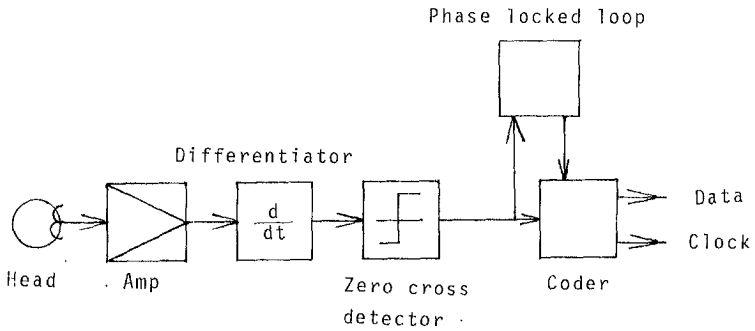


Fig. 8 MFM Detection Circuit

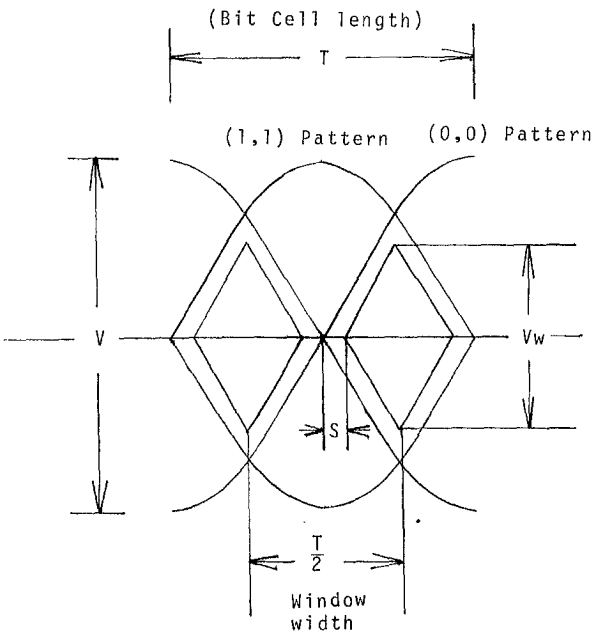
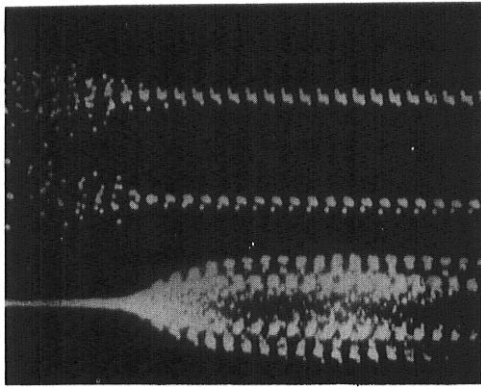


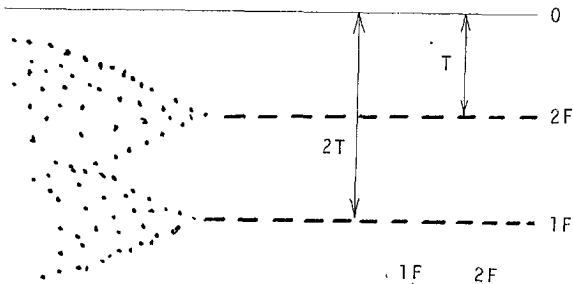
Fig. 9 Eye Pattern and Window Width



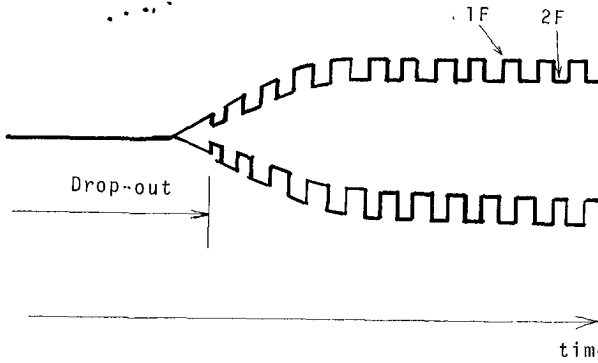
(a)

(b)

0.5 msec/div



(c)



(d)

Fig. 10 Resolution and Peak Shift During a Drop-out.

Normalized number

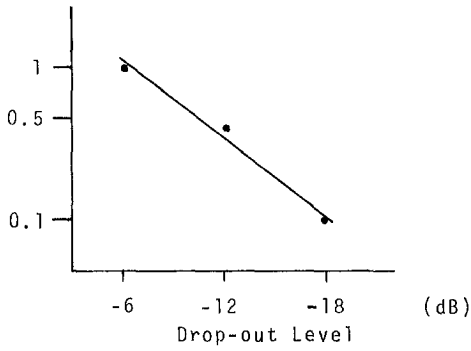


Fig. 11 Normalized Drop-out Number vs Drop-out Level

Burst length

(Frame)

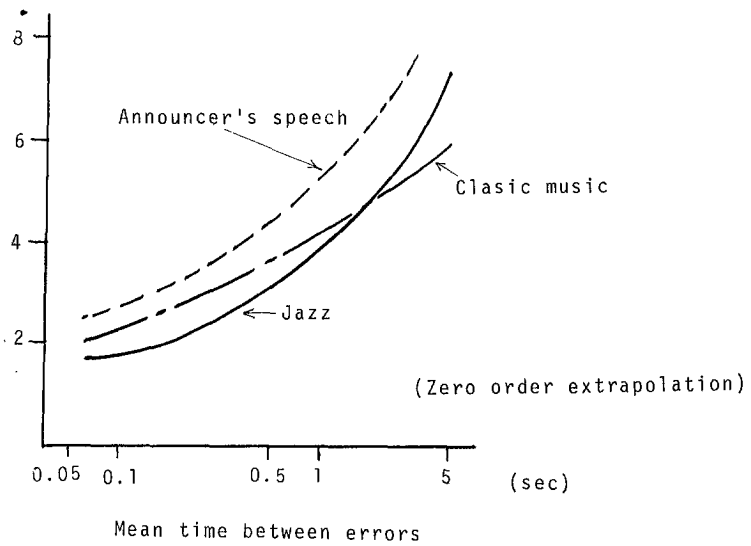


Fig. 12 Subjective Impairment of Error Concealment

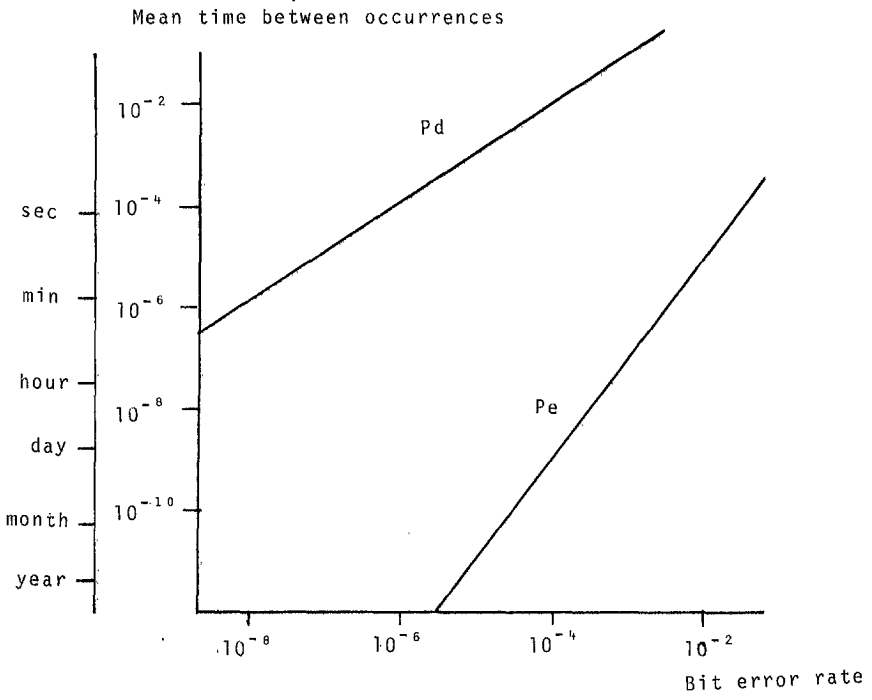


Fig. 13 Pd and Pe vs p

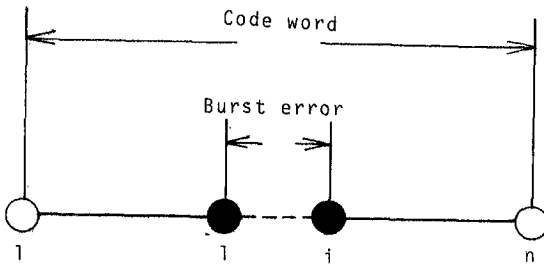


Fig. 14 Burst Error